**Astronomy
&
Astrophysics**

Orbits of new Hipparcos binaries. II[*],[**]

I. I. Balega[1], Y. Y. Balega[1], K.-H. Hofmann[2], E. V. Malogolovets[1], D. Schertl[2],
Z. U. Shkhagosheva[1], and G. Weigelt[2]

[1] Special Astrophysical Observatory, N.Arkhyz, Zelenchuk region, 369167 Karachai-Cherkesia, Russia
e-mail: balega@sao.ru
[2] Max-Planck-Institut für Radioastronomie, Auf dem Hügel 69, 53121 Bonn, Germany

ABSTRACT

We continue the presentation of new orbits for Hipparcos binaries determined from regular speckle interferometric observations. Most of the data were collected in the period between 1998.77 and 2004.82 using the 6 m BTA telescope of the Special Astrophysical Observatory in Zelenchuk. New orbits are presented for six pairs: HIP 4809, HIP 4849, HIP 5531, HIP 19206, HIP 105947, and HIP 114922. One of the pairs, HIP 114922, has M dwarf components orbiting with a period of 19.72 yr. Two binaries, HIP 4809 and HIP 5531, have luminosity class IV components. The periods of the orbits range from 7.30 yr to 28.99 yr. All of the orbits can be considered definitive; however, the total mass error for the systems remains high, mainly due to Hipparcos parallax error.

Key words. stars: binaries: visual – stars: fundamental parameters – stars: late-type

1. Introduction

This is the second in a series of publications presenting the orbits of new binary stars discovered during the Hipparcos mission (ESA 1997). Over 500 measurements of 180 new Hipparcos pairs were made between 1998.77 and 2004.82 with the speckle interferometer at the 6 m BTA telescope of the Special Astrophysical Observatory in Zelenchuk, Russia. The study focused primarily on nearby pairs of spectral types from late F to M. The relative astrometry for our volume-limited sample of Hipparcos binary stars is given in the first papers of this series (Balega et al. 2002, 2004, 2005, hereafter Papers I, II, and III). A fraction of these systems display clear Keplerian motion of more than $20-30°$/yr in position angle θ and/or $10-20$ mas/yr in separation ρ. Due to the high precision of speckle observations, typically $0.5°$ in θ and 1.5 mas in ρ, the data are sufficient for calculating first orbits for about 20 such systems. In addition to the relative positions, the obtained magnitude differences become important clues for deriving the physical properties of the components.

In the preceding paper (Balega et al. 2005, hereafter Paper IV), 6 orbits were given for G to M type Hipparcos pairs at distances of 15 to 66 pc from the Sun. In this new paper, we report the results for 6 additional binaries of similar spectral types and distances. To derive the orbits, we used the already published speckle observations, supplemented with new measurements from the 6 m BTA telescope. For each pair, the data set consists of 9 to 15 independent measurements, including the first Hipparcos discovery.

2. Observations and binary star orbits

Our observational technique is described in Paper I of this series. Both the visual and infrared data from the 6 m telescope were used to define the orbits. The visual data were processed using the software developed at the Special Astrophysical Observatory, while the diffraction-limited image reconstructions in the infrared were performed at the Max-Planck-Institut fuer Radioastronomie in Bonn. Our speckle interferometric measurements made between 2001 and 2004 have not yet been published and are given here for those pairs under study for the first time.

The orbital elements were estimated using the Monet (1977) method, together with the differential correction of preliminary elements. All of the BTA observations were given unit weights. Horch et al. (1999, 2002) and Mason et al. (1999, 2001) measurements were taken with the weights 0.6 and 0.5, respectively, following the aperture ratio of the telescopes, namely, 6:3,5 and 6:2,5. The Hipparcos relative positions for the epoch 1991.25 were given 0.5 weights; however, in two cases, HIP 5531 and 114922, the Hipparcos astrometric data were rejected because of large errors. The position angles θ were reduced to a common equinox 2000.0.
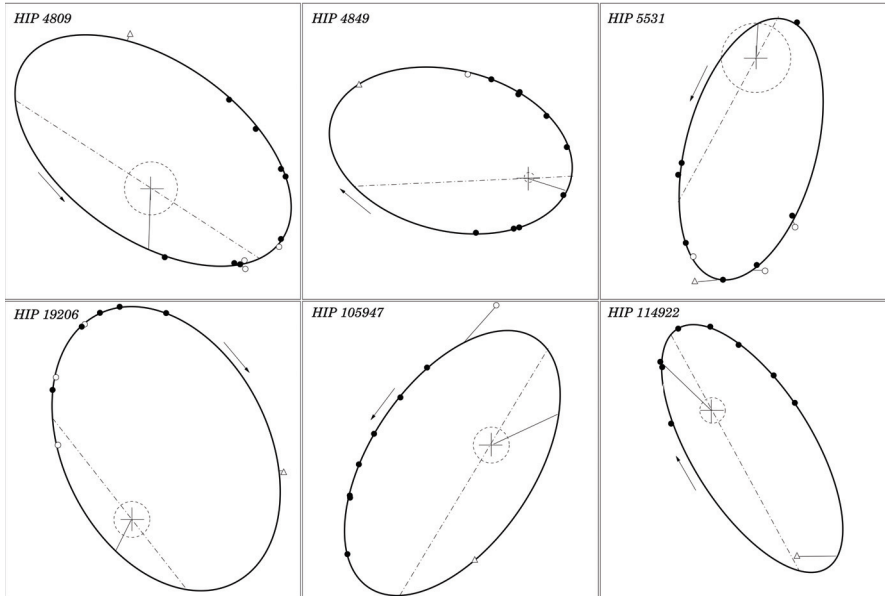
The results of our orbit calculations are presented in Table 1, where the first column gives the HIP number of the object, and the subsequent columns list, respectively, the

---

[*] Based on observations made with the 6-m BTA telescope, which is operated by the Special Astrophysical Observatory, Russia.
[**] Appendices A and B are only available in electronic form at http://www.edpsciences.org

Table 1. Orbital elements for six Hipparcos binaries.

HIP	P (yr)	σ_P	T	σ_T	e	σ_e	a (mas)	σ_a	i (deg)	σ_i	Ω (deg)	σ_Ω	ω (deg)	σ_ω	σ_Θ (deg)	σ_ρ (mas)
4809	16.41	0.11	1998.62	0.02	0.393	0.012	128	2	58.4	0.5	57.1	0.8	106.9	0.6	0.8	2
4849	28.99	0.58	2002.68	0.01	0.678	0.005	465	7	144.3	0.8	92.6	2.2	205.4	1.9	1.0	3
5531	7.30	0.11	1995.71	0.11	0.720	0.008	87	2	54.7	1.5	151.6	1.3	219.1	1.4	1.4	2
19206	21.33	0.44	1996.77	0.08	0.686	0.011	223	6	122.2	1.2	38.2	1.7	255.6	1.1	0.9	2
105947	18.79	0.57	1993.96	0.40	0.354	0.010	168	3	57.1	2.1	149.1	1.5	129.7	6.4	0.3	1
114922	19.72	0.16	1999.81	0.02	0.440	0.003	219	2	117.1	0.3	28.6	0.5	324.8	0.7	0.3	1

Fig. 1. Apparent ellipses representing the orbital elements for HIP 4809, HIP 4849, HIP 5531, HIP 19206, HIP 105947, and HIP 114922. The BTA speckle data are indicated by filled circles, other interferometric data by open circles, and Hipparcos first measurements by triangles. Residual vectors for all measures are plotted, but in most cases, they are smaller than the points themselves. The orbital motion direction is indicated by an arrow. The solid line shows the periastron position, while the dot-dashed line represents the line of nodes. North is up and east is to the left. The dashed circle at the position of the brighter component has a radius of 0.02″.

period P (in years), periastron passage T, eccentricity e, semi-major axis a of the true orbit (in milliarcseconds), orbit inclination i (in degrees), position angle of the node Ω (in degrees, refers to the epoch 2000.0), and the longitude of periastron ω (in degrees), together with their formal errors. The last two columns give the rms deviation of θ and ρ measurements from a solution that excludes the high-residual observations mentioned in the next section.

Following the Worley & Heintz (1983) grading scheme (orbital coverage, separation residuals, no large gaps in position angle measurements), the presented orbits can be evaluated as grade 2, "good" (most of a revolution, well-observed, and with sufficient curvature of the motion) or grade 3, "reliable" (at least half of the orbit well defined). The orbits of HIP 105947 and HIP 114922 are the best of these 6 systems, while the HIP 4849 orbit shows the largest deviations. Tables A.1 to A.6 of the Appendix A summarize the speckle observations and the residuals of position angles θ and separations ρ from the determined orbital elements. The first observations were taken from the Hipparcos Catalogue (ESA 1997).

The projection of the new set of orbits on the plane of the sky is presented in Fig. 1, in which our speckle measurements are plotted as filled circles, while other speckle measurements are shown as open circles. The Hipparcos 1991.25 discoveries are indicated by triangles.

In the late 1990's, optical and infrared speckle interferometry became an effective technique for measuring accurate
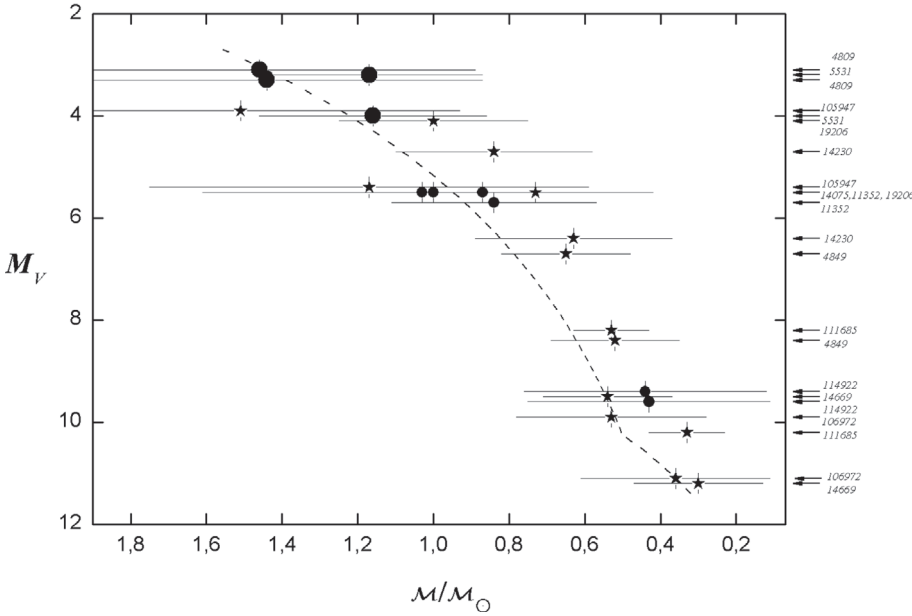
brightness ratios for binary and multiple stars. We decided to include the existing magnitude difference measurements for our six systems in this paper. Table B.1 of Appendix B lists 30 Δm values obtained with the 6 m BTA telescope, together with 14 measurements appearing in the literature. The six 1991.25 measurements are the Hipparcos first observations (Hp filter, $\lambda/\Delta\lambda = 476/210$ nm). Not one of the objects is noted as potentially variable in the Hipparcos Catalogue.

Table 2 lists the derived basic physical properties and the main orbital parameters of the observed systems, including the 6 new Hipparcos binaries from Paper IV. For convenience, we have included the Hipparcos parallaxes and their standard deviations in Cols. 2 and 3 of the table. Column 4 gives the absolute magnitudes for the components derived from the mean speckle interferometric magnitude differences, total V magnitudes of the systems from the SIMBAD database, and π_{hp}. For these nearby stars, we assumed no absorption ($A_V = 0$). Column 5 presents the corresponding spectral types for the luminosity class V stars. The exceptions are HIP 4809 and 5531, which have luminosity class IV components. For them, the spectral types were inferred from their color indices. Columns 6 to 10 give the periods of the systems in years, semi-major axes in AU, total masses from Kepler's third law, and standard deviations of the total masses found as

$$\frac{\sigma_\mathcal{M}}{\mathcal{M}} = \left[9\left(\frac{\sigma_a}{a}\right)^2 + 4\left(\frac{\sigma_P}{P}\right)^2 + 9\left(\frac{\sigma_\pi}{\pi}\right)^2\right]^{1/2} .$$

Table 2. Main parameters of the orbits, properties of the components, and total masses for 12 new Hipparcos binaries. Six pairs with new orbits from Paper IV are also included.

HIP	π_{hp}	σ_π	M_V		$S p$		P	a	$\mathcal{M}$	$\sigma_\mathcal{M}$	$\sigma_\mathcal{M}/\mathcal{M}$
	mas	mas	A	B	A	B	yr	AU	$\mathcal{M}_\odot$	$\mathcal{M}_\odot$	%
4809	13.94	0.90	3.1	3.3	G6–G9IV		16.41	9.18	2.90	0.57	20
4849	46.61	1.61	6.7	8.4	K3	K8	28.99	9.77	1.17	0.14	12
5531	17.41	0.67	3.2	4.0	G0IV		7.30	5.00	2.33	0.30	13
11352	23.19	1.21	5.5	5.7	G8	G9	6.85	4.31	1.71	0.27	16
14075	15.17	1.44	5.5	5.5	G8	G8	13.89	7.07	2.03	0.58	29
14230	29.62	1.09	4.7	6.4	G2	K2	5.91	3.71	1.47	0.26	18
14669	64.83	4.26	9.5	11.2	M2	M4	28.31	8.78	0.84	0.17	20
19206	24.00	0.92	4.1	5.5	G0	G8	21.33	9.29	1.75	0.25	14
105947	17.11	1.13	3.9	5.4	F8	G8	18.79	9.82	2.68	0.58	22
106972	39.78	3.70	9.9	11.1	M2	M4	18.57	6.74	0.89	0.25	28
111685	52.94	1.94	8.2	10.2	K7	M3	16.77	6.23	0.86	0.10	12
114922	31.50	3.85	9.4	9.6	M1	M2	19.72	6.95	0.87	0.32	37

Fig. 2. Location of the components of 12 new Hipparcos binaries from Table 2 on the mass-luminosity diagram. Binaries with $\Delta m \leq 1$ are plotted as filled circles, while those with $\Delta m > 1$ are plotted as stars. The larger circles indicate two systems with evolved components, HIP 4809 and HIP 5531. Error bars are taken the same as for the mass sums in Table 2. The dashed line represents the empirical $\mathcal{M}/L$ relation from Henry & McCarthy (1993).

The last column in the table presents the total mass error in percent. Note that the semi-major axes of the orbits lie in the narrow range between 3.7 and 9.8 AU, which indicates the area of efficiency of speckle interferometry for the study of a nearby sample of Hipparcos binaries.

Comparison of $\sigma_\mathcal{M}/\mathcal{M}$ in Table 2 with the Hipparcos parallax relative error $(\sigma_\pi/\pi)_{hp}$ leads to the conclusion that the mass-sum error is linearly increasing with $(\sigma_\pi/\pi)_{hp}$:

$$\sigma_\mathcal{M}/\mathcal{M} = 3[1 + (\sigma_\pi/\pi)_{hp}](\text{per cent}).$$

Hence, with more precise parallaxes in the future (one may envision the GAIA astrometric mission), the quality of our orbits will be sufficient for deriving masses with an accuracy of about 5%.

Figure 2 shows the location of the components of 12 binaries from Paper IV and the present study on the $\mathcal{M}/L$ diagram. To derive the mass ratios q for all but two systems, we used the empirical mass-luminosity relation for main-sequence

dwarfs from Henry & McCarthy (1993), which is plotted as a dashed line in the figure. In the cases of HIP 5531 and 19206, we used the q values from spectroscopic surveys (Nordström et al. 2004). The pairs with small magnitude differences are marked by filled circles, and those with $\Delta m > 1$ mag are plotted as stars. The larger filled circles represent the evolved components of HIP 4809 and 5531.

The components of several binaries (HIP 19206, 14230, 4849, 111685) are noticeably deviant from the $\mathcal{M}/L$ fits towards smaller masses. Note that all of them belong to systems with $\Delta m > 1$ mag. The difference between the locus of the $\mathcal{M}/L$ relation and our results can be explained by the different evolutionary stages and metallicities of the stars. However, because of the limited size of the sample, the effects of age and metallicity were not considered. The most probable reasons for the deviations are the mass-sum errors. A small change in the parallax value can shift the obtained mass sums towards the main region of the empirical $\mathcal{M}/L$ diagram. For example, a π_{hp}

reduction from 24 mas to 22 mas will put the componets of HIP 19206 exactly on the $\mathcal{M}/L$ curve; the same is true if one takes $\pi = 27$ mas in place of $\pi_{hp} = 30$ mas for HIP 14230.

In Fig. 2, the mass-sum error bars for the binaries in the upper part of the diagram are significantly wider than for the low-mass pairs. This difference is explained by a smaller relative error of parallaxes for the nearby low-mass dwarfs.

For two systems from Paper IV, HIP 14669 and 106972, we obtained significantly larger dynamical parallaxes π_{dn} compared to the Hipparcos parallaxes, correspondingly, $\pi_{dn} = 69.86$ mas instead of $\pi_{hp} = 64.83$ mas and $\pi_{dn} = 44.85$ mas instead of $\pi_{hp} = 39.78$. Both of these systems have faint M-type components. Dynamical parallaxes for other pairs agree well with the Hipparcos parallaxes, giving a difference of $1-2$ mas.

3. Comments on individual systems

3.1. HIP 4809 = HD 6009

The mean Δm value from speckle and Hipparcos measurements, collected in Table B.1, is 0.14 mag in the V-band with a standard error of 0.03 mag. Here we supposed that Δm does not change significantly in the range $\lambda 545-800$ nm. The only measurement in the K-band within the error gives the same value. With this magnitude difference in hand, we used the Hipparcos parallax value $\pi_{hp} = 13.94 \pm 0.90$ mas and $V = 6.71$ from the SIMBAD database to obtain absolute magnitudes for the components $M_A = 3.1$ and $M_B = 3.3$. Together with the color $(B - V) = 0.783 \pm 0.007$ given in the Hipparcos catalog, this corresponds to G6–G9 type subgiant stars. This estimate agrees with the luminosity class given by Yoss (1961) from his analysis of the strength of the $\lambda 4077$ ionized strontium line based on the prism spectra from the Curtis Schmidt telescope of the University of Michigan and slit spectrograms from the 60 inch reflector of the Mt. Wilson Observatory. The luminosity class IV for the components is also supported by the moderate cyanogen absorption at $\lambda 4216$.

The orbit was defined from 16 astrometric measurements, including the first resolution by Hipparcos, one observation by Mason et al. (2001) with the 2.1 m telescope of the McDonald Observatory (0.06″ resolution limitation), two observations by Horch et al. (2002) with the 3.5 m WIYN telescope at Kitt Peak, and 12 observations with the 6 m BTA telescope. To obtain a consistent orbit, we had to adjust the quadrants of θ measurements from the 2.1 m and the 3.5 m telescopes. The quadrant of the first Hipparcos is also inconsistent with the majority of further speckle observations, which can be explained by the low value of the magnitude difference and the larger-than-typical error on the Hipparcos ΔH_p magnitude. The mean value of residuals for the BTA speckle measurements is 0.4 mas in ρ and 0.5° in θ. However, despite small residuals of the measurements, the total mass error for the system is 20%, which is explained by the overwhelming input of the π_{hp} error.

3.2. HIP 4849 = HD 6101 = GJ 3071

The total proper motion of this nearby system, listed in the Lowell Observatory survey as G 1-43, is $\mu = 0.41''$/yr

(Giclas et al. 1961). Based on these data, Sandage & Kowal (1986) included GJ 3071 in the list of possible new nearby subdwarfs. However, it was found that the measured $U - B = +0.86$ for G 1-43 at the given $B - V = +1.01$ color does not deviate from the corresponding Hyades $U - B$ value, and, consequently, the star cannot be a subdwarf. In his compilation survey for stars that may be within 25 pc of the sun, Halliwell (1979) first mentioned the discordant photometric and trigonometric parallaxes for the star, which could be a sign of its binary nature.

After the first resolution of the system by Hipparcos in 1991.25, eleven speckle measurements covered about 2/3 of the visual orbit. One speckle observation belongs to Mason et al. (2001), while all others are from the 6 m BTA telescope. With an orbital period of 29 years, this pair has the largest semi-major axis of the visual orbit among the binaries listed in Table 1.

3.3. HIP 5531 = HD 6840

This is a high proper motion star with $\mu_\alpha = 0.25''$/yr. The common color index of the system $B - V = 0.553 \pm 0.005$, taken from the SIMBAD database (the Hipparcos measurement), corresponds to a G0 spectral type. Chen et al. (2000), Lambert & Reddy (2004), and Nordström et al. (2004) determined its effective temperature from the reddening-corrected $b - y$, c_1 and m_1 indices in the range $\log T_e = 3.7670 - 3.7679$ corresponding to an early G-dwarf. However, the photometric distance determination ($\pi_{ph} = 37$ mas) is not in agreement with the Hipparcos parallax $\pi_{hp} = 17$, suggesting evolved components. From our mean magnitude difference in Table B.1, $\Delta m = 0.68$, the absolute magnitudes of the stars in the pair are $M_A = 3.21$ and $M_B = 3.89$, respectively. The authors cited above find the metallicity for HIP 5531 in the range of $-0.62 \leq [Fe/H] \leq -0.44$. Given the T_e, M_V, and [Fe/H] for the star, an age of 7 Gyr is estimated for the main component by interpolation among the evolutionary tracks provided by Girardi et al. (2000).

Due to good phase coverage of the interferometric orbit, the period and semi-major axis of HIP 5531 are well-defined. Note that 2/3 of its total mass error comes from the Hipparcos parallax error. Recently, HIP 5531 was recognized to be also a SB2 with a mass ratio 0.99 ± 0.02 (Nordström et al. 2004). With an accuracy of about 10%, the subsequent individual masses of the components are $\mathcal{M}_A = 1.17\,\mathcal{M}_\odot$ and $\mathcal{M}_B = 1.16\,\mathcal{M}_\odot$. The next periastron passage for HIP 5531 will be in the beginning of 2010. To obtain more accurate masses and luminosities for the components, it is worth keeping the binary in the lists of future spectroscopic and interferometric monitorings.

3.4. HIP 19206 = HD 26040

Spectral type G0V results from the Eggen (1985) and Nordström et al. (2004) photometry that gives $(b - v) = 0.36$ and $\log T_e = 3.772$. This relates to the main component of the system because the secondary is 1.34 mag fainter, as follows from our Table B.1. For the secondary, our differential photometry leads to $M_B = 5.5$ and spectral type G8V.

The system is also given as SB2 in the Nordström et al. (2004) survey of F and G dwarfs in the Solar neighborhood. The mass ratio $q = 0.73 \pm 0.11$ from this paper fits well with our $q = 0.80$ arising from the masses of dwarfs of the corresponding spectral types.

3.5. HIP 105947 = HD 204236

The distribution of speckle observations along the apparent ellipse is uneven, with most measurements concentrated near the apastron. Therefore, following the criteria of Worley & Heintz (1983), the orbit must be graded only as "reliable". The Mason et al. (1999) speckle point of 1997.7 falls well outside the apparent ellipse after assigning the right quadrant; hence, it was ignored in the calculations.

3.6. HIP 114922 = GJ 893.4

This high proper-motion star is also known as Vyss 860. Absolute magnitudes for the components were calculated with the assumption that $\Delta m_R = 0.2$. Apart from the first Hipparcos observation, all other measurements define a reliable ellipse of the visual orbit. Note that two speckle measurements were obtained with the 6 m telescope just at the moment of periastron passage in 1999.8. The Hipparcos parallax of this faint system is given with an accuracy of only 12.2%. As a consequence, the mass-sum is defined with a standard error of 37% (input of the $\sigma_{\pi_{\mathrm{hp}}}$ error in the muss-sum error exceeds 99%).

4. Summary

We have presented new speckle measurements of the angular separations ρ and position angles θ of the components of 6 new Hipparcos binaries, and derive new orbits and masses based upon Hipparcos parallaxes and relative speckle astrometry obtained between 1997−2004. For all of the six systems, in Table B.1 we present Δm measurements from the 6 m telescope in the wavelength range of $\lambda = 545$ nm to $\lambda = 2115$ nm. For comparison, the Hipparcos ΔV_{Hp} differences and Horch et al. (2004) Δm measurements are also included. These differential magnitudes allow the absolute magnitudes and spectral types of the components to be determined.

The mass-sum accuracies for the 6 new systems range between 12 and 37%. The dominant source of uncertainty in the overall error budget for the masses remains the parallax in all cases. For example, in the case of HIP 114922, 99% of the total error comes from the π_{hp} error.

Two systems, HIP 4809 and 5531, have evolved components. In addition, HIP 5531 was recently found to be SB2 with a mass ratio of 0.99 (Nordström et al. 2004). Because of the even phase coverage of speckle observations and the relatively short orbital period, this pair has the most accurate speckle orbit among the studied systems. Another pair given as SB2 by Nordström et al. (2004) is HIP 19206. The physical parameters of these two binaries can be significantly improved when the spectroscopic orbits become available.

The final result is the obtained location of the components on the "mass-absolute magnitude" diagram. New Hipparcos binaries with orbits from Paper IV of this series are also plotted. Most of the dwarf systems fall close to the empirical relation of Henry & McCarthy (1993), but with four "outliers" due to large relative mass-sum errors.

About half of the components in Table 2 have masses between 0.20 and 0.50 $\mathcal{M}_\odot$. As mentioned by Henry et al. (1999), this region of the diagram is perhaps more poorly determined than the lower masses. They explain this peculiarity by the large scatter of the empirical data on the plateau in the $\mathcal{M}/L$ relation caused by the effects of hydrogen molecules in the atmospheres combined with the deep convective regions. In addition, substantial progress in defining the bottom of the $\mathcal{M}/L$ diagram has been made recently because of the special attention given to the study of brown dwarfs and planets in multiple systems. Our observational goal is to define the relative orbits for a few dozen new Hipparcos binaries with an accuracy of semimajor axes better than 1%. New spectroscopic radial velocities and chemical compositions from the 6 m telescope will allow us to improve the orbital elements and the knowledge of the physical properties of the components.

References

Balega, I. I., Balega, Y. Y., Hofmann, K.-H., et al. 2002, A&A, 385, 87 (Paper I)
Balega, I. I., Balega, Y. Y., Maksimov, A. F., et al. 2004, A&A, 422, 627 (Paper II)
Balega, I. I., Balega, Y. Y., Maksimov, A. F., et al. 2005, Bull. Special Astrophys. Obs., 59 (Paper III)
Balega, I. I., Balega, Y. Y., Hofmann, K.-H., et al. 2005, A&A, 433, 591 (Paper IV)
Chen, Y. Q., Nissen, P. E., Zhao, G., et al. 2000, A&AS, 141, 491
Eggen, O. J. 1985, PASP, 97, 807
ESA 1997, The Hipparcos and Tycho Catalogues, ESA SP-1200
Giclas, H. L., Burnham, R., & Thomas, N. G. 1961, Lowell Obs. Bull., 5, 61
Girardi, L., Bressan, A., Bertelli, G., & Chiosi, C. 2000, A&AS, 141, 371
Halliwell, M. J. 1979, ApJS, 41, 173
Henry, T. J., & McCarthy, D. W. 1993, AJ, 106, 773
Henry, T. J., Franz, O. G., Wasserman, L. H., et al. 1999, ApJ, 512, 864
Horch, E. P., Ninkov, Z., van Altena, W. F., et al. 1999, AJ, 117, 548
Horch, E. P., Robinson, S. E., Meyer, R. D., et al. 2002, AJ, 123, 3442
Horch, E. P., Meyer, R. D., & van Altena, W. F. 2004, AJ, 127, 1727
Lambert, D. L., & Reddy, B. E. 2004, MNRAS, 349, 757
Mason, B. D., Martin, C., Hartkopf, W. I., et al. 1999, AJ, 117, 1890
Mason, B. D., Hartkopf, W. I., Holdenried, E. R., & Rafferty, T. J. 2001, AJ, 121, 3224
Monet, D. G. 1977, ApJ, 214, L133
Nordström, B., Mayor, M., Andersen, J., et al. 2004, A&A, 418, 989
Pluzhnik, E. A. 2005, A&A, 431, 587
Sandage, A., & Kowal, C. 1986, AJ, 91, 1140
Yoss, K. M. 1961, ApJ, 134, 809
Worley, C. E., & Heintz, W. D. 1983, Publ. USNO, 24, part 7

Online Material

Appendix A: Hipparcos and speckle relative astrometry of six new binaries, and residuals

Table A.1. HIP 4809.

Epoch	θ	ρ	$\Delta\theta$	$\Delta\rho$	Reference
1991.250	8.0	0.118	–1.5	0.004	ESA (1997)
1998.772	189.5	0.050	0.1	0.000	Paper I
1999.747	228.2	0.086	–0.1	–0.001	Paper I
1999.813	229.5	0.088	–0.3	0.000	Paper II
1999.823	229.7	0.094	–0.3	0.005	Mason et al. (2001)
1999.888	232.5	0.089	1.1	–0.002	Horch et al. (2002)
2000.767	245.5	0.107	–1.4	0.001	Horch et al. (2002)
2000.873	249.2	0.106	0.7	0.000	Paper III
2000.876	248.8	0.106	0.2	0.000	Paper III
2001.753	261.9	0.107	0.2	0.000	Paper III
2001.753	261.9	0.107	0.2	0.000	Paper III
2001.753	262.2	0.107	0.5	0.000	this paper
2001.845	263.1	0.107	0.0	0.000	this paper
2002.726	275.2	0.103	–2.0	0.002	this paper
2002.796	278.6	0.100	0.2	–0.001	this paper
2003.928	299.9	0.092	0.3	–0.001	this paper
2004.815	318.7	0.090	0.6	0.000	this paper

Table A.2. HIP 4849.

Epoch	θ	ρ	$\Delta\theta$	$\Delta\rho$	Reference
1991.250	62.0	0.711	–0.4	0.000	ESA (1997)
1997.718	31.4	0.433	–0.1	–0.007	Mason et al. (1999)
1998.772	21.4	0.376	0.1	0.003	Paper I
1999.747	7.3	0.302	–0.5	–0.005	Paper I
1999.813	6.6	0.305	0.1	0.003	Paper II
2000.876	342.7	0.231	0.8	0.000	Paper III
2001.753	307.8	0.182	–0.6	–0.001	Paper III
2002.736	245.6	0.146	–1.7	0.002	this paper
2002.799	245.1	0.141	2.8	–0.001	this paper
2003.788	169.1	0.178	–0.4	0.002	this paper
2003.928	162.9	0.188	0.2	0.000	this paper
2004.815	135.2	0.275	–0.1	–0.002	this paper

Table A.3. HIP 5531.

Epoch	θ	ρ	$\Delta\theta$	$\Delta\rho$	Reference
1991.250	165.0	0.136	–4.6	0.004	ESA (1997)
1997.630	162.8	0.122	1.5	0.001	Horch et al. (1999)
1998.774	171.9	0.131	0.3	–0.001	Paper I
1999.634	182.6	0.125	3.4	0.001	Horch et al. (2002)
1999.821	180.4	0.121	–0.7	0.000	Paper II
2000.765	193.3	0.102	0.6	0.004	Horch et al. (2002)
2000.878	193.1	0.095	–1.5	0.001	Paper III
2002.796	310.4	0.032	0.4	0.001	this paper
2003.788	145.0	0.075	1.2	0.002	this paper
2003.928	146.8	0.082	–0.4	0.000	this paper
2004.816	159.5	0.116	–0.6	–0.003	this paper

Table A.4. HIP 19206.

Epoch	θ	ρ	$\Delta\theta$	$\Delta\rho$	Reference
1991.250	287.0	0.178	–1.4	0.005	ESA (1997)
1997.830	44.5	0.116	–1.7	0.001	Horch et al. (1999)
1998.772	31.2	0.169	0.2	–0.001	Paper I
1999.012	28.0	0.179	–0.5	–0.001	Horch et al. (2002)
2000.759	13.5	0.224	–1.2	0.002	Horch et al. (2002)
2000.876	14.2	0.223	0.2	–0.001	Paper III
2001.753	8.5	0.234	–0.1	0.001	Paper III
2002.797	3.0	0.238	0.5	0.001	this paper
2004.824	350.4	0.234	–0.3	0.000	this paper

Table A.5. HIP 105947.

Epoch	θ	ρ	$\Delta\theta$	$\Delta\rho$	Reference
1991.250	172.0	0.127	0.1	–0.001	ESA (1997)
1997.720	357.6	0.151	–17.8	0.037	Mason et al. (1999)
1998.780	39.2	0.108	–0.4	0.001	Paper I
1999.745	62.2	0.110	0.0	–0.001	Paper I
2000.864	84.6	0.127	0.1	0.001	Paper III
2001.752	98.5	0.143	0.4	0.000	Paper III
2002.799	110.0	0.163	–0.4	–0.001	this paper
2002.799	110.7	0.163	0.2	–0.001	this paper
2004.815	127.5	0.195	–0.1	0.000	this paper

Table A.6. HIP 114922.

Epoch	θ	ρ	$\Delta\theta$	$\Delta\rho$	Reference
1991.250	210.0	0.256	−10.5	−0.033	ESA (1997)
1998.774	108.4	0.065	0.0	0.001	Paper I
1999.742	48.7	0.099	0.0	−0.003	Paper I
1999.815	46.2	0.107	−0.1	0.001	Paper II
2000.864	21.9	0.134	0.5	0.000	Paper III
2001.845	0.5	0.127	−0.5	0.001	this paper
2002.736	337.8	0.108	0.2	−0.002	this paper
2003.927	299.6	0.108	0.1	0.001	this paper
2004.815	275.3	0.126	−0.1	0.000	this paper
2004.821	275.2	0.126	−0.1	0.000	this paper

Appendix B: Magnitude differences for six new Hipparcos binaries

Table B.1. Speckle interferometric magnitude differences and Hipparcos ΔHp (HMA04 = Horch et al. 2004; P05 = Pluzhnik 2005).

HIP	Date	Δm	$\lambda/\Delta\lambda$, nm	Ref.
4809	1991.25	0.28 ± 0.41	V_{Hp}	ESA (1997)
	1998.77	0.17 ± 0.15	545/30	Paper I
	1998.77	0.10 ± 0.24	545/30	P05
	1999.75	0.30 ± 0.16	2115/214	Paper I
	1999.81	0.19 ± 0.04	610/20	Paper II
	1999.89	0.05 ± 0.15	648/41	HMA04
	2000.77	0.22 ± 0.15	503/40	HMA04
	2000.87	0.12 ± 0.19	800/110	Paper III
	2000.87	0.16 ± 0.05	600/30	Paper III
	2001.75	0.00 ± 0.12	545/30	Paper III
	2001.75	0.00 ± 0.12	600/30	Paper III
4849	1991.25	1.87 ± 0.04	V_{Hp}	ESA (1997)
	1998.77	1.72 ± 0.04	610/20	Paper I
	1999.75	0.78 ± 0.12	2115/214	Paper I
	1999.81	1.66 ± 0.05	610/20	Paper II
	2000.88	1.66 ± 0.03	600/30	Paper III
	2001.75	1.48 ± 0.03	600/30	Paper III
	2001.75	1.48 ± 0.03	600/30	Paper III
5531	1991.25	0.47 ± 0.24	V_{Hp}	ESA (1997)
	1997.63	0.73 ± 0.08	648/41	HMA04
	1998.77	0.71 ± 0.03	545/30	Paper I
	1998.77	0.73 ± 0.03	545/30	P05
	1999.63	0.45 ± 0.15	601/42	HMA04
	1999.82	0.75 ± 0.03	610/20	Paper II
	2000.76	0.88 ± 0.08	648/41	HMA04
	2000.88	0.71 ± 0.02	545/30	Paper III
19206	1991.25	1.32 ± 0.24	V_{Hp}	ESA (1997)
	1997.83	1.37 ± 0.08	648/41	HMA04
	1998.77	1.42 ± 0.04	610/20	Paper I
	1999.01	1.33 ± 0.08	648/41	HMA04
	2000.76	1.29 ± 0.08	648/41	HMA04
	2000.88	1.39 ± 0.02	545/30	Paper III
	2001.75	1.26 ± 0.02	600/20	Paper III
105947	1991.25	1.17 ± 0.60	V_{Hp}	ESA (1997)
	1998.78	1.50 ± 0.06	545/30	Paper I
	1998.78	1.50 ± 0.04	545/30	P05
	1999.75	1.16 ± 0.14	2115/214	Paper I
	2000.86	1.40 ± 0.02	545/30	Paper III
	2001.75	1.29 ± 0.05	850/75	Paper III
	2001.75	1.31 ± 0.06	600/30	Paper III
114922	1991.25	0.44 ± 0.57	V_{Hp}	ESA (1997)
	1998.77	0.00 ± 0.35	800/60	Paper I
	1999.82	0.16 ± 0.09	800/60	Paper II
	2000.86	0.00 ± 0.23	800/110	Paper III